Applied Scientific Research **52:** 309–329, 1994.

On Predicting Particle-Laden Turbulent Flows*

S. ELGHOBASHI
Mechanical and Aerospace Engineering Department, University of California, Irvine, CA 92717, U.S.A.

Received 6 May 1993; accepted in revised form 17 October 1993

Abstract. The paper provides an overview of the challenges and progress associated with the task of numerically predicting particle-laden turbulent flows. The review covers the mathematical methods based on turbulence closure models as well as direct numerical simulation (DNS). In addition, the statistical (pdf) approach in deriving the dispersed-phase transport equations is discussed. The review is restricted to incompressible, isothermal flows without phase change or particle-particle collision. Suggestions are made for improving closure modelling of some important correlations.

1. Introduction

The objective of this paper is to review the mathematical approaches currently employed in predicting particle-laden turbulent flows. The word 'particles' hereinafter denotes, for brevity, solid particles, liquid droplets or gaseous bubbles, dispersed in a carrier flow.

Perhaps it is helpful to emphasize, at the outset, the two challenges facing the attempts of numerically predicting particle-laden turbulent flows:

(i) A significant feature of these flows, and notably the major stumbling block preventing their detailed solution and our full physical understanding of them, is the presence of a very wide spectrum of important length and time scales. These scales are associated with the microscopic physics of the dispersed phase in addition to those of the fine and large structures of turbulence. Current and anticipated computer technology does not allow the simultaneous resolution of the large scale motion and of the flow around all individual dispersed particles. The resolution of such disparate scales must be performed via independent numerical simulations of the smallest (particle) scale motions. This information is then incorporated into the simulation of larger scales.

(ii) Despite the numerous efforts devoted to the study of turbulence in particle-free flows (i.e. single-phase fluid flow) over the past seven decades the understanding of the physics of turbulence remains incomplete as indicated by the limited success (e.g. lack of universality) of the current mathematical models of turbulence. This fact sets the *upper limit* to the current understanding of the *more complex* particle-laden turbulent flows.

* Lecture presented at a workshop on turbulence in particulate multiphase flow, Fluid Dynamics Laboratory, Battelle Pacific Northwest Laboratory, Richland, WA, March 22–23, 1993.

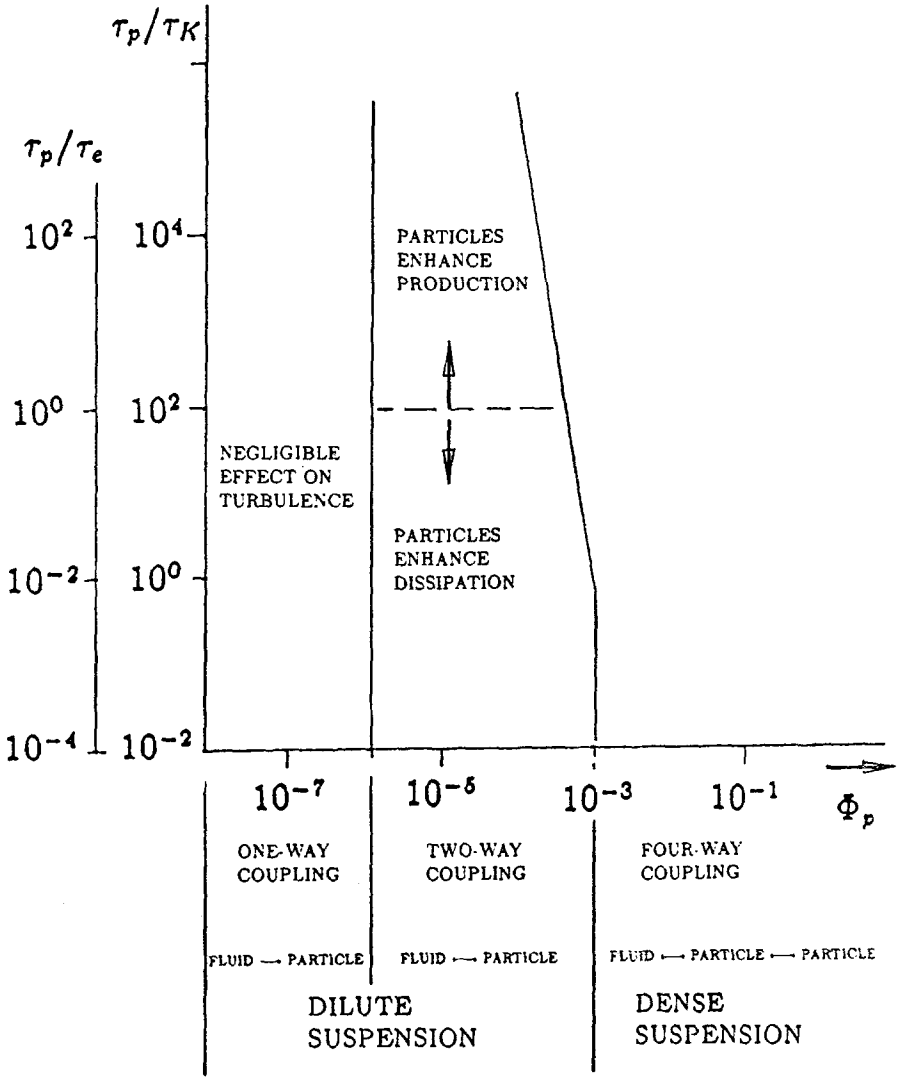

Fig. 1. Map of regimes of interaction between particles and turbulence.

These two challenges resulted in the development of mathematical treatments with different levels of sophistication to predict these flows. The following sections provide a brief review of these methods. It should be emphasized that the ultimate validation of any of these methods is determined by comparing the predictions with data from *well-defined* experiments with *acceptable quality*.

In an earlier review [8], particle-laden turbulent flows were classified from the point of view of the type of interaction between the particles and turbulence. The classification map of [8] is modified slightly and presented in Figure 1. The quantities on the dimensionless coordinates are defined below.

Φ_p: volume fraction of particles, $\Phi_p = MV_p/V$
M: number of particles
V_p: volume of a single particle
V: volume occupied by particles and fluid
d: diameter of particle
τ_p: particle response time $= \rho_p d^2/(18\rho_f \nu)$ for Stokes flow
τ_K: Kolmogorov time scale $= (\nu/\varepsilon)^{1/2}$
τ_e: turnover time of large eddy $= \ell/u$

In the above definitions, ρ is the material density and the subscripts p and f denote respectively the particle and carrier fluid. ν is the kinematic viscosity of the fluid. ℓ is the length scale of the energy containing eddies, u is the rms fluid velocity, and ε is the dissipation rate of turbulence kinetic energy. For very low values of Φ_p ($\leq 10^{-6}$) the particles have negligible effect on turbulence, and the interaction between the particles and turbulence is termed as **one-way coupling**. This means that particle dispersion, in this regime, depends on the state of turbulence but due to the negligible concentration of the particles the momentum transfer from the particles to the turbulence has an insignificant effect on the flow. In the second regime, $10^{-6} < \Phi_p \leq 10^{-3}$, the momentum transfer from the particles is large enough to alter the turbulence structure. This interaction is called **two-way coupling**. Now, in this regime and for a given value of Φ_p, lowering τ_p (e.g. smaller d for the same particle material and fluid viscosity) increases the surface area of the particulate phase, hence the increased dissipation rate of turbulence energy. On the other hand, as τ_p increases for the same Φ_p, the particle Reynolds number, R_p, increases and at values of $R_p \geq 400$ vortex shedding takes place resulting in enhanced production of turbulence energy. The vertical coordinate (τ_p/τ_e) is related to the other coordinate (τ_p/τ_K) via the turbulence Reynolds number ($R_\ell = u\ell/\nu$) since $(\tau_e/\tau_K) = R_\ell^{1/2}$. Thus the coordinates shown are for $R_\ell = 10^4$, which is typical in practical flows. Flows in the two regimes discussed above are often referred to as dilute suspensions. In the third regime, because of the increased particle loading, $\Phi_p > 10^{-3}$, flows are referred to as dense suspensions. Here, in addition to the two-way coupling between the particles and turbulence, particle/particle collision takes place, hence the term **four-way coupling**. As Φ_p approaches 1, we obtain a **granular flow** in which there is no fluid, and obviously that flow is beyond the scope of this review.

The difference between the map in Figure 1 and that in [8] is that now the line separating the two-way and four-way coupling regimes is inclined whereas it was vertical in the earlier map. This is intended to indicate the tendency of particle-particle collision to take place at higher values of τ_p/τ_e, thus transforming the two-way to four-way coupling regime.

The behavior of particles in turbulent flows with one-way coupling is reasonably understood, at least in unconfined homogeneous flows. The limitation to this understanding, as mentioned earlier, stems mainly from the incomplete understanding of turbulence itself even in particle-free flows. On the other hand, flows in the two-way or four-way coupling regimes are still at the infancy stage of understanding due to the highly nonlinear nature of the interactions in these flows.

The mathematical approaches to be reviewed here can be classified into those based on *turbulence closure models* and those of *direct numerical simulation (DNS)* of turbulence. The latter solves the instantaneous three-dimensional Navier–Stokes equations of the carrier flow directly, resolving *all* the scales of turbulence, thus eliminating the need for closure approximations.

We restrict the present discussion to isothermal incompressible fluids without phase changes (e.g. vaporization) or chemical reaction. Also, the effects of particle-particle of particle-wall collisions are not considered here.

2. Mathematical Methods Based on Closure Models

Currently there are two approaches for modeling particle-laden turbulent flows, namely the two-fluid (two-continuum) and the Lagrangian (or particle trajectory) methods. Within the two-fluid approach there are two different methods for deriving the transport equations for the dispersed phase, one *deterministic* and the other *statistical*. The following subsections describe briefly these approaches and highlight some recent developments and areas that need model improvements.

2.1. The Two-Fluid Approach

2.1.1. *Deterministic Method for Both Phases*

In the two-fluid approach, the particulate phase is considered, under certain conditions [9], as a continuum having conservation equations similar to those of the carrier flow. The instantaneous equations describing the conservation of mass and momentum for each 'fluid' are

$$\frac{\partial \rho^k}{\partial t} + \nabla \cdot (\rho^k \mathbf{U}^k) = 0, \tag{1}$$

$$\frac{\partial \rho^k \mathbf{U}^k}{\partial t} + \nabla \cdot (\rho^k \mathbf{U}^k \mathbf{U}^k) = \nabla \cdot (\Phi_k \boldsymbol{\tau}^k) + \rho^k \mathbf{g} + (-1)^k \mathbf{F}. \tag{2}$$

In the above equations, the superscript k is an index for the phase; $k = 1$ for the carrier flow, and $k = 2$ for the particulate phase. Also the subscript k denotes either the fluid, f, or the particulate phase, p and $\rho^1 = \rho_f \Phi_f$, and $\rho^2 = \rho_p \Phi_p$. $\mathbf{U}$ is the velocity vector, $\boldsymbol{\tau}$ is the stress tensor which includes the pressure and viscous stresses for each phase, $\mathbf{g}$ is the gravitational acceleration, and $\mathbf{F}$ is the two-way coupling force per unit volume. Note that the term containing $\mathbf{F}$ has opposite signs

for the two phases, and that $\Phi_p + \Phi_f = 1$ by definition. It is important to note that for $k = 2$, the quantities $\mathbf{U}$, τ and $\mathbf{F}$ are associated with *the cloud of particles* present in a unit volume and *not with a single particle*. In other words, Equations (1) and (2) are obtained for a single realization of the flow field by averaging over a control volume that is much larger than the particle size and much smaller than the characteristic length of the flow field. This is just as for $k = 1$, the velocity $\mathbf{U}$ for the carrier fluid represents the average of the instantaneous velocities of a large number of molecules contained within a small fluid element.

The stress tensor τ for the particular phase accounts for three interactions, namely:

(i) the influence of the surrounding particles on the relative velocity $(u_{pi} - u_{fi})$ of an individual particle,
(ii) particle-particle collisions, and
(iii) pressure gradient in the carrier flow itself.

(i) and (ii) are important only for dense suspensions ($\Phi_p > 10^{-3}$), otherwise negligible. The viscous stress of the particle phase originates only from (i). As the distances between the particles decreases ($\leq 10d$), the presence of their rigid boundaries alters the flow field around them, thus modifying the relative velocity distribution around each particle [18]. This modification changes all the forces imparted on each particle. Some of these forces are purely viscous, such as the viscous drag and lift. Thus the viscous stresses occur once there is relative motion between the fluid and closely-spaced particles, and are clearly different from the Reynolds stresses which result from the random motion of the particles.

Since it is not possible with current supercomputer or massively parallel computer technology to directly solve (1) and (2) using DNS for high Reynolds number turbulent flows in practical engineering flows, one of the options available at present is to average these equations, leading to the inevitable closure problem.

There are two possible methods of averaging (1) and (2), namely a volume-fraction (or spatial density) weighted average and a non-weighted time-average. The latter is the well known Reynolds averaging. A volume-fraction weighted velocity $\langle U_i^k \rangle$ is defined as

$$\langle U_i^k \rangle = \frac{\langle U_i^k \Phi_k \rangle}{\langle \Phi_k \rangle} .$$

If the material density ρ_k is constant then $\langle U_i^k \rangle$ is also mass-weighted. The type of averaging employed has serious consequences on the number and order of the resulting correlations, and hence the effort required to model them. For example, if mass-weighted averaging is adopted, the two correlations $\langle \phi u_i \rangle$ and $\langle \phi u_i u_j \rangle$ are identically zero, where the lower case symbols denote the difference between the instantaneous and the mass-weighted values of the variable. This in contrast to time-averaging the unweighted variables where these two correlations are finite and thus require modeling. The distinction between these two types of averaging is quite similar to the distinction between Favre averaging and Reynolds averaging of

variable density single-phase flows. Reeks [26, 27, 28] provides details of modeling the mass-weighted averaged equations for the dispersed phase. Now, we focus on the difficulties arising from time-averaging (1) and (2).

The first difficulty is the evaluation of the correlation $\langle \phi u_i \rangle_p$ which results from the second term in (1), where lower case symbols denote fluctuations, and $\langle \ldots \rangle$ indicate time-averaging. This correlation represents a turbulent flux of ϕ_p in the x_i direction. In the case of dilute suspensions, sometimes this correlation is assumed negligible since $\Phi_p \ll 1$. However, if gradient transport is used, $\langle \phi u_i \rangle_p = -D_{\phi,i}(\partial \Phi_p / \partial x_i)$, two new problems arise. The first is to evaluate the turbulent diffusivity $D_{\phi,i}$ of the 'cloud of particles'. And even if $D_{\phi,i}$ is determined by assuming a relation between the diffusivities of particle and fluid, which in itself is not a trivial task, a gradient transport may be appropriate only if $\tau_p \ll \tau_e$ and may fail to mimic the turbulent dispersion of the particle cloud in general. For example, near the nozzle exit of a particle-laden jet, the radial gradient $(\partial \Phi_p / \partial r)$ would be quite large yet the lateral flux $\langle \phi u_i \rangle_p$ is known to be negligible there. Furthermore, the phenomenon of 'crossing trajectories', by which a particle, due to its own inertia or the action of an external field, follows a path different from its surrounding fluid [35, 6, 13], is independent of $(\partial \Phi_p / \partial r)$. The 'crossing trajectories' effect reduces particle dispersion in the directions *normal* to the particle path even if $(\partial \Phi_p / \partial x_i)$ is large in these directions. Thus, the evaluation of $\langle \phi u_i \rangle_p$ requires careful examination, especially for larger values of Φ_p in the two-way and four-way coupling regimes where $\langle \phi u_i \rangle_p$ is not negligible. It is evident that the pdf approach discussed in the next subsection has more physical realism in evaluating this correlation than gradient transport. It should also be noted that DNS results [14], provide detailed information to assess the validity of current and improved models.

The difficulty in modeling the time-averaged momentum equation of the particulate phase stems mainly from two quantities, namely $\langle u_i u_j \rangle_p$ and $\langle \phi u_i u_j \rangle_p$. It has been shown by Elghobashi and Abou Arab [9] that the third order correlation $\langle \phi u_i u_j \rangle_p$ can be modeled in terms of the two second order correlations $\langle \phi u_i \rangle_p$ and $\langle u_i u_j \rangle_p$. Now, the physical meaning of the corresponding correlation for the carrier flow $\langle u_i u_j \rangle_f$, is generally accepted as a 'turbulent stress' per unit mass resulting from a 'lump of fluid' initially moving with velocity u_i in the direction x_i being pushed in the normal direction x_j with a velocity u_j, thus exchanging momentum with the new host fluid. In dilute suspensions, with two-way coupling, all momentum exchanges occur only due to fluid-fluid or fluid-particle interactions. Consider two volume elements at time t, each containing particles in different configurations as shown in Figure 2. The rms velocity fluctuations of the two ensembles are different. At time $t + \delta t$, the two ensembles, due to their different rms velocities, approach each other as shown in the figure. We see that the momentum within each volume element experiences a change due to the fact that individual particles with different rms velocities cross their initial volume boundaries. It is then possible to interpret the second-order correlation $\langle u_i u_j \rangle_p$ as a mechanism for momentum

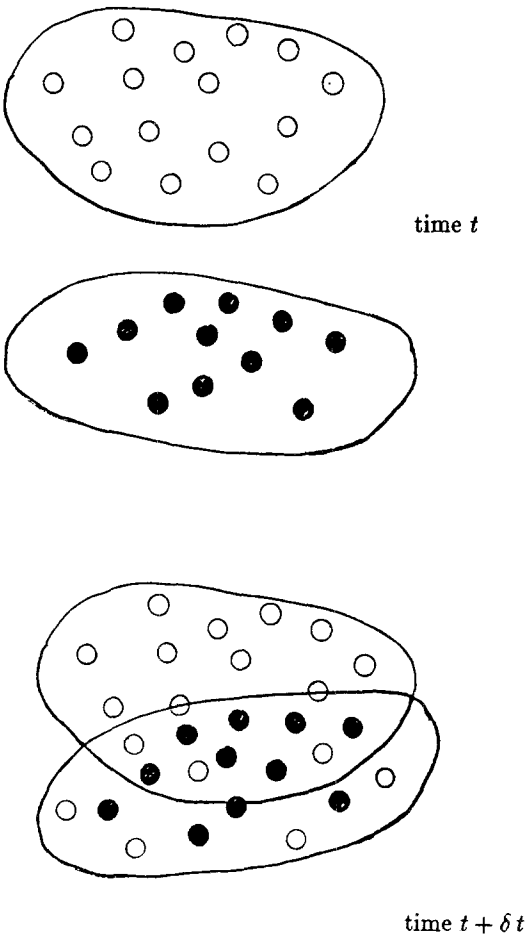

Fig. 2. Momentum transfer between two ensembles of dispersed phase in a turbulent flow.

transfer between two ensembles within the dispersed phase, and by analogy to the carrier flow it can be called a Reynolds stress for the dispersed phase. However, there is conceptual difficulty in extending this analogy to model $\langle u_i u_j \rangle_p$ as a product of an eddy viscosity and a gradient of the mean velocity of the dispersed phase. The reason for the difficulty is that particle crossing the volume boundaries can be completely independent of the gradients of U_p. In general, the transfer of momentum from the carrier flow to the particles and external forces (e.g., gravity or electromagnetic field) control the motion of the particles. Thus, it is unjustified to derive a transport equation for the kinetic energy of turbulence $1/2\langle u_i u_i \rangle_p$ of the particulate phase in which the production term equals $\langle u_i u_j \rangle_p (\partial U_i / \partial x_j)_p$. It is clear that modeling $\langle u_i u_j \rangle_p$ requires a rigorous analysis that is lacking at present. It is expected that DNS results would provide the needed information to assess the validity of current models and suggest improvements. In addition, analytical

studies similar to that of Hwang and Shen [16] (1989) may be helpful.

The k and ε Equations with Two-Way Coupling. The closure problem discussed briefly above indicates the need for additional transport equations to provide information about the local length- and time-scales of turbulence. In the present discussion, the dependent variables for these additional equations are the turbulent kinetic energy, k, and its rate of dissipation ε. Although it is possible to derive the transport equations for the Reynolds stresses $\langle u_i u_j \rangle$ [19] for the carrier flow, including the two-way coupling terms, the lack of understanding of the relevant physical phenomena of the two-way interactions and the unavailability of detailed experimental data render the closure of these equations highly qualitative at best.

The exact transport equations for the carrier flow turbulence kinetic energy k and its dissipation rate ε in the two-way coupling regime have been derived in [9]. A quantity that describes the effects of the particles on k and ε is the second-order correlation $\langle u_{fi}(u_{pi} - u_{fi}) \rangle$. In order to evaluate this correlation, Elghobashi and Abou Arab [9] used Chao's solution [4] of the linearized equation of particle motion and proposed the following model:

$$\langle u_{fi}(u_{pi} - u_{fi}) \rangle = -(1/2)\langle u_{fi}^2 \rangle \left[1 - \int_0^\infty \frac{\Omega_1 - \Omega_R}{\Omega_2} f(\omega)\, \mathrm{d}\omega \right], \tag{3}$$

where Ω_1, Ω_2 and Ω_R are functions of the turbulence frequency, ω, ρ_f, ν, ρ_p and d. The exact forms of these functions are given in [9]. Now the validity of the model presented in (3) has been examined only indirectly by comparing the predicted time-averaged correlations, like the turbulent stresses, $\langle u_{fi} u_{fj} \rangle$, with their measured values in a turbulent particle-laden jet by Elghobashi *et al.* [10]. What is needed is a direct evaluation of the term on the right hand side of (3) by using DNS results. This will provide validation of the model described by (3). Models of the other terms in the energy and dissipation equations can also be evaluated. It is also interesting to note that $\langle u_{fi}(u_{pi} - u_{fi}) \rangle$ was classified in [9] as '*extra dissipation*'. It was believed that this quantity would most probably be always negative because either (a) the fluid and particle velocities have, on the average, the same sign, hence their correlation, $\langle u_{fi} u_{pi} \rangle$, would be positive but its magnitude would be less than the fluid autocorrelation $\langle u_{fi} u_{fi} \rangle$; or (b) the velocities u_{fi} and u_{pi}, have on the average different signs, then the whole quantity is negative regardless of the relative magnitudes of the correlations. However, the recent DNS results [14] indicate that it is possible that u_{fi} and u_{pi} have on the average the same sign and $\langle u_{fi} u_{pi} \rangle$ is larger than $\langle u_{fi} u_{fi} \rangle$. In that study [14], the turbulence was decaying and a sufficient concentration of particles, with sufficient inertia was 'dragging' the surrounding fluid along, resulting in a positive value of the correlation $\langle u_{fi} u_{pi} \rangle$, hence a source of energy. Thus it is recommended here to reclassify the correlation $\langle u_{fi}(u_{pi} - u_{fi}) \rangle$ as an *extra source/sink* of energy due to particle/fluid interaction.

2.1.2. *Statistical Method for the Dispersed Phase*

The basic assumption that the dispersed phase behaves as a continuum remains invoked here, but the governing equations of that phase are derived from the transport equation of the probability density function (pdf) [26].

Let $W(\mathbf{v}, \mathbf{x}, t)$ be the instantaneous pdf for a particle with velocity $\mathbf{v}$ and position $\mathbf{x}$ at time t, and $\langle W(\mathbf{v}, \mathbf{x}, t)\rangle$ be the average pdf in the phase space for N identical statistically independent particles, where $\langle \ldots \rangle$ denotes ensemble averaging. Thus

$$N = \int \langle W(\mathbf{v}, \mathbf{x}, t)\rangle \, \mathrm{d}\mathbf{v} \, \mathrm{d}\mathbf{x}. \tag{4}$$

The spatial number density $\langle n(\mathbf{x}, t)\rangle$ of these particles at $\mathbf{x}$ and t is

$$\langle n(\mathbf{x}, t)\rangle = \int \langle W(\mathbf{v}, \mathbf{x}, t)\rangle \, \mathrm{d}\mathbf{v}. \tag{5}$$

Given the volume of a single particle V_p, the instantaneous volume fraction $\Phi_p(\mathbf{x}, t)$ of the particle cloud at $\mathbf{x}$ and t is

$$\Phi_p(\mathbf{x}, t) = V_p \langle n(\mathbf{x}, t)\rangle. \tag{6}$$

The distribution of velocities $\psi(\mathbf{v}, \mathbf{x}, t)$ of the particles within the cloud at $\mathbf{x}$ and t is

$$\psi(\mathbf{v}, \mathbf{x}, t) = \frac{\langle W(\mathbf{v}, \mathbf{x}, t)\rangle}{\langle n(\mathbf{x}, t)\rangle}. \tag{7}$$

Thus

$$\int \psi(\mathbf{v}, \mathbf{x}, t) \, \mathrm{d}\mathbf{v} = 1. \tag{8}$$

If $\theta(\mathbf{v}, \mathbf{x}, t)$ is some function of particle velocity at $\mathbf{x}$ and t, then the mean property $\Theta(\mathbf{x}, t)$ at $\mathbf{x}$ and t is given by

$$\Theta(\mathbf{x}, t) = \int \theta(\mathbf{v}, \mathbf{x}, t)\psi(\mathbf{v}, \mathbf{x}, t) \, \mathrm{d}\mathbf{v}. \tag{9}$$

Also

$$\langle n(\mathbf{x}, t)\rangle \Theta(\mathbf{x}, t) = \int \theta(\mathbf{v}, \mathbf{x}, t)\langle W(\mathbf{v}, \mathbf{x}, t)\rangle \, \mathrm{d}\mathbf{v}, \tag{10}$$

$$= \langle n\theta(\mathbf{v}, \mathbf{x}, t)\rangle. \tag{11}$$

Similarly, the statistical moments of $\mathbf{v}$ of the order $(k + l)$ are calculated from

$$\langle v_i^k v_j^l\rangle(\mathbf{x}, t) = \int v_i^k v_j^l \psi(\mathbf{v}, \mathbf{x}, t) \, \mathrm{d}\mathbf{v}, \tag{12}$$

$$= \frac{\langle n v_i^k v_j^l(\mathbf{x}, t)\rangle}{\langle n(\mathbf{x}, t)\rangle}. \tag{13}$$

Thus, once $\langle W(\mathbf{v},\mathbf{x},t)\rangle$ is known one can obtain all the statistics that depend on the velocity and volume fraction of the cloud of particles. Marble [21] derived the continuity and momentum equations of the dispersed phase from the Boltzmann equation but did not account for the effects of turbulence. More recently, Andresen [1] followed Marble's approach to derive the transport equations for the dispersed phase including the Reynolds stresses and higher moments. He also proposed a modified Maxwellian pdf to complete the closure of the equation set. However, Andresen [1] included only the effects of particle-particle collisions and not particle-eddy interactions.

Buyevich [3] used the Fokker–Planck equation (FPE), of the Brownian motion, to derive the transport equations for dispersed phase. Reeks [26] pointed out that the original FPE is only appropriate for a particle with a Markovian random motion, i.e. the particle response time is much greater than that of the carrier flow, $\tau_p \gg \tau_e$. Consequently, FPE fails to preserve the random Galilean transformation (RGT). Reeks [26] modified the original FPE to ensure RGT invariance, and thus becomes appropriate for *all* particle response times. RGT is achieved by imposing on the carrier flow a translational velocity, uniform in space and time invariant, but randomly varying in magnitude from one realization to the next. When RGT invariance is applied to the carrier flow turbulence, it ensures the correct spectral energy transfer across the wave number space. The general form of FPE for $\langle W\rangle$ is

$$\left(\frac{\partial}{\partial t}+\mathbf{v}\cdot\frac{\partial}{\partial \mathbf{x}}-\beta\,\frac{\partial}{\partial \mathbf{v}}\cdot\mathbf{v}\right)\langle W\rangle=-\frac{\partial}{\partial \mathbf{v}}\cdot\mathbf{J}, \tag{14}$$

where β is a dissipative tensor, generally anisotropic, whose reciprocal, β_{ij}^{-1}, represents the particle response time for a change of its velocity in the i-direction due to a change in the carrier flow velocity in the j-direction. The significant modification of FPE by Reeks [26] is in the new form of the phase space diffusion current $\mathbf{J}$ which represents the net acceleration imparted to the particle due to its interaction with turbulent eddies. The new form of $\mathbf{J}$ which preserves RGT invariance is

$$\mathbf{J}=-\left(\frac{\partial}{\partial \mathbf{v}}\cdot\boldsymbol{\mu}+\frac{\partial}{\partial \mathbf{x}}\cdot\boldsymbol{\lambda}+\boldsymbol{\gamma}\right)\langle W\rangle, \tag{15}$$

where $\boldsymbol{\mu}$, $\boldsymbol{\lambda}$ and $\boldsymbol{\gamma}$ are dispersion tensors whose components are memory integrals along particle trajectories, and depend on the fluctuations in the velocity and position of a particle about $\mathbf{v}$ and $\mathbf{x}$ over time scales of the order of that of the carrier flow velocity mean and fluctuations. The tensor $\boldsymbol{\gamma}$ is zero in homogeneous turbulence. Reeks [27] derived the conservation equations of mass, momentum, Reynolds stresses, and turbulence kinetic energy of the dispersed phase from the appropriate moments of his modified FPE taken over all particle velocities. The mass and momentum conservation equations are similar in form to (1) and (2) but their closure can be achieved if $\langle W(\mathbf{v},\mathbf{x},t)\rangle$ is known. One of the important findings of Reeks [27] is that the dispersed phase does not behave as a simple

Newtonian fluid. For example, the dispersed phase Reynolds stress depends on the local gradients in both the mean velocity of the carrier flow as well as that of the dispersed phase itself, with both contributions of nearly the same order. More recently, Reeks [28] applied this method to the dispersion of particles in a simple shear flow. He showed that the Reynolds stresses are composed of a *homogeneous component*, as if the carrier flow is homogeneous, and a *deviatoric component* due to the mean shear gradient. The eddy viscosity approximation ignores the homogeneous component in the shear stresses and accounts only for the viscous contribution in the deviatoric component. Obviously such information can be used to improve closure models of the dispersed phase equations. Perhaps it is useful to summarize the advantages of the pdf approach as follows:

(i) Closure in phase space is at a more basic level of the dynamics so probably has a greater chance of success than closure applied directly to the momentum and Reynolds stress transport equations;
(ii) Simple Boussinesq approximations at the phase space level do not necessarily imply simple Boussinesq approximations for the Reynolds stresses;
(iii) Closure approximation is required for only one term namely the net acceleration due to particle interactions with the turbulent motions as opposed to two closure approximations in the momentum equation namely for the Reynolds stresses and the inter-phase momentum coupling term;
(iv) It establishes a natural length scale (mean free path) which when compared with the dimensions of the flow sets a criterion for the validity of simple gradient diffusion;
(v) It is the only way to formulate the correct boundary conditions since these involve information about the velocity distribution at the walls.

2.2. The Lagrangian Approach

In this approach [36, 15], the conservation equations governing the motion of the carrier flow (continuity, momentum, k and ε) are integrated over a fixed mesh covering the flow domain as in the two-fluid approach. The particulate phase is represented by a number of *computational particles* whose trajectories $\mathbf{x}_p(t)$ are computed by simultaneously integrating:

$$\frac{\mathrm{d}\mathbf{x}_p}{\mathrm{d}t} = \mathbf{u}_p, \tag{16}$$

and the equation of particle motion which is generally written as [23]:

$$\begin{aligned} m_p(\mathrm{d}u_{pi}/\mathrm{d}t_p) \;=\; & m_p(u_{fi} - u_{pi})/\tau_p \\ & + m_f(Du_{fi}/Dt) \\ & + \frac{1}{2}\, m_f(Du_{fi}/Dt - \mathrm{d}u_{pi}/\mathrm{d}t_p) \end{aligned}$$

$$+ 6a^2(\pi\rho\mu)^{1/2} \int_{t_{p0}}^{t_p} \frac{\mathrm{d}/\mathrm{d}\tau(u_{fi} - u_{pi})}{(t_p - \tau)^{1/2}}\, \mathrm{d}\tau$$

$$+ (m_p - m_f)g_i$$

$$+ \frac{1}{2}(\pi\rho a^2)C_L L_i V^2. \tag{17}$$

Equation (17) describes the balance of forces acting on the particle as it moves along its trajectory. The term on the left hand side is the inertia force acting on the particle due to its acceleration. The terms on the right side are respectively the forces due to viscous and pressure drag, fluid pressure gradient and viscous stresses, inertia of virtual mass, viscous drag due to unsteady relative acceleration (Basset), buoyancy, and Saffman's lift force due to shear in the carrier flow [31, 30]. C_L is the lift coefficient evaluated by Saffman; L_i are the three x_i direction cosines; and V is the magnitude of the relative velocity vector. It should be mentioned here that this form of Saffman's lift force is quite restricted by the condition that $R_s \ll R_g^{1/2}$, where $R_s = |v_r|d/\nu$ and $R_g = Gd^2/\nu$; G is the gradient of fluid velocity. The recent work by McLaughlin [25] removes that restriction and provides a new form of the lift force. Also, the above form of the Basset force is strictly correct when the *instantaneous velocity* of the particle at injection (time = 0) is exactly equal to that of the surrounding fluid; a condition that is possible *only* in numerical simulations. For arbitrary initial particle velocity, Maxey [22] showed that an additional term is needed to account for the initial drag resulting from the mismatch between the two velocities.

In order to integrate (17), the instantaneous velocity of the carrier flow needs to be known at the particle position. Since only the time-averaged velocity of the fluid is known at the fixed points of the computational grid, an assumption must be made to obtain the instantaneous velocity from its time-averaged value, $\langle u_{fi} \rangle$ and k. The most widely used method is to compute the rms velocity at the Eulerian mesh point using a Gaussian pdf with zero mean and a variance that corresponds to k. The instantaneous velocity of the fluid at the mesh point is calculated by adding this rms velocity to the time-mean value there. This method produces isotropic fluid velocity fluctuations at each point. A particle passing within a *prescribed zone* surrounding the mesh point is assumed to encounter this instantaneous velocity. Outside this zone a new velocity is computed, i.e., the particle experiences a *step change* in the value of the instantaneous fluid velocity. The size of the prescribed zone is usually taken equal to the length scale of the energy containing eddies at the Eulerian mesh point.

More recently, Berlemont *et al.* [2] proposed a method that avoids this discontinuity in the fluid velocity along the particle path. In that method, the trajectory of a discrete particle 'P' and that of fluid point 'F' coinciding with it initially (time = 0) are computed simultaneously. The two trajectories differ, as shown in Figure 3, due

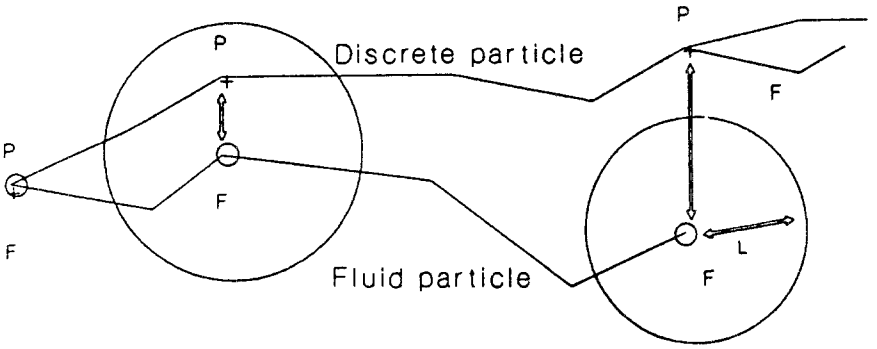

Fig. 3. Time development of the trajectories of a discrete particel 'P' and a fluid point 'F', initially coincident (from Berlemont *et al.*, 1990).

to the crossing trajectories effect. A velocity-correlation domain (shown as a circle in the figure) associated with the fluid point, F, is prescribed. The extent of that domain in the x_i-direction is $L_i = u_{fi}\tau_{L_i}$, where u_{fi} is the fluctuating velocity, τ_{L_i} is the Lagrangian integral time-scale computed from an assumed shape of the temporal correlation function:

$$R_{ij}(\tau) = \frac{\langle u_{fi}(t)u_{fi}(t+\tau)\rangle}{\sqrt{\langle u_{fi}^2(t)\rangle}\sqrt{\langle u_{fj}^2(t+\tau)\rangle}} . \tag{18}$$

with no summation on i or j, $i, j = 1, 2, 3$. The distances $|\mathbf{x}_{pi} - \mathbf{x}_{fi}|$ between P and F in the three directions x_i are then compared with L_i. When one of these distances is greater than the corresponding L_i, a new fluid point is released at the current position of P. In effect, the method computes the fluid velocity fluctuation $u_{fi}(t)$ at P from

$$u_{fi}(t+\delta t) = u_{fj}(t)\beta_{ij} + d_i, \tag{19}$$

where δt is the time step of the integration scheme. The coefficients β_{ij} and d_i are functions of R_{ij}. The main objective is to insure that the fluid velocity fluctuation at the particle location satisfies the velocity covariance matrix obtained from the Eulerian solution. The vector d_i accounts for randomness during time δt and is a Gaussian random vector with zero mean, and the tensor β_{ij} represents randomness during previous time and depends on the local Eulerian covariances. Details of the relations between β_{ij}, d_i and R_{ij} are included in the study by Zhou and Leschziner [37].

In general, the difficulties in the Lagrangian approach are as follows. First, there are severe limitations to the particle equation (17). Specifically, this equation:

(i) is valid only for the Reynolds number $R_p \ll 1$ and $d \ll \eta$, where η is the Kolmogorov length scale, thus the interesting case in which the particle is of comparable size to an eddy cannot be accurately treated. At present, only a

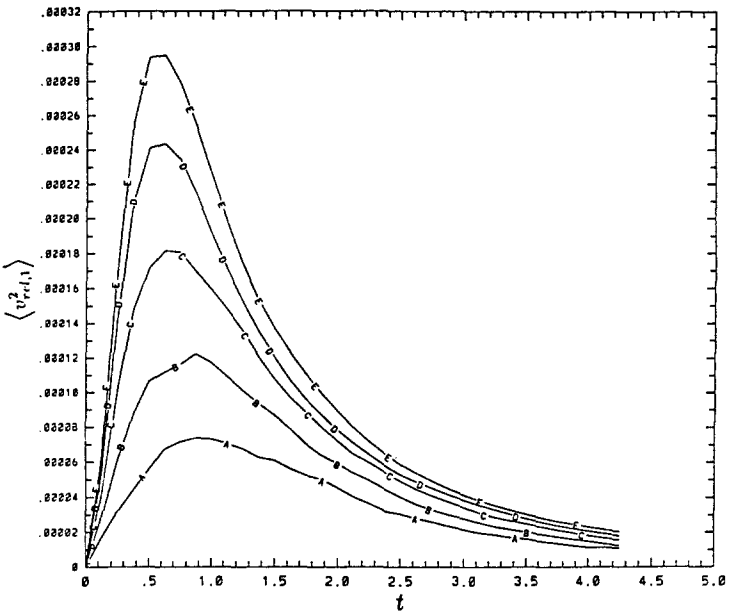

Fig. 4. Effect of the ratio of real to computational particles on the time development of the mean square relative velocity between the particles and carrier flow (Elghobashi and Truesdell, 1992).

numerical solution of the full Navier–Stokes equations can predict the flow and the resulting forces on the particle in such cases. A numerical solution has been obtained recently for the time-dependent, three-dimensional flow of a cylindrical vortex interacting with a spherical particle of comparable size. The results provide details of the temporal variation of the drag and lift forces for $R_p \leq 100$ [17].

(ii) does not account for the effect of the neighboring particles on the motion of the particle of interest, and

(iii) does not account for the two-way coupling effects, i.e., the effect of particles on the fluid, especially the term (Du_{fi}/Dt). Only numerical solutions of Navier–Stokes equations around one or more particles can provide such information [18].

The second difficulty has been discussed recently by MacInnes and Bracco [20] who demonstrated that several Lagrangian models do not preserve the divergence properties of the imposed mean flow. The method of sampling the fluctuation velocity in these models leads to a spurious component of mean velocity, causing anomalous drifting of the particles relative to the mean flow.

The third difficulty is that due to computer limitations, all the Lagrangian methods compute the trajectories of only a fraction of the real particles. If the number of real particles is M_r and that of the computational particles is M_c,

then the ratio (M_r/M_c) is always $\gg 1$. For example, if $\Phi_p = 10^{-3}$, and the particle diameter $d = 200\ \mu$, then $M_r \approx 10^9/\text{m}^3$. If M_c equals 10^4, then each computational particle represents 10^5 real particles. And since the instantaneous concentration of particles at a given position represents the probability that a number of particles exist at that position as discussed in the preceding section, a diminished probability cannot be predicted since the ratio (M_r/M_c) is always constant. As an illustration, consider a laboratory experiment to measure the radial profiles of particle concentration in a turbulent jet downstream of the injection nozzle. It is quite possible to find that there is *only one* particle on the average (long time-average) at a large radial distance from the center line. Numerically, the arrival of one computational particle at that position is exactly equivalent to the arrival of M_r real particles, and thus higher concentrations than that actually measured. In other words, in the numerical example presented above, the arrival of one particle at a given position always brings with it 10^5 particles, whereas the real vanishingly small probability may correspond to a number that is orders of magnitude smaller. Figure 4 shows results of DNS to assess the dependence of mean square relative velocity, $\langle u_{\text{rel}}^2 \rangle = \langle (u_{fi} - u_{pi})^2 \rangle$, on the ratio (M_r/M_c) for $\Phi_p = 2.5 \times 10^{-4}$ in homogeneous isotropic turbulence. The values of (M_r/M_c) for the curves A, B, C, D or E are respectively 932, 477, 217, 97 and 51. The reason for the reduction of $\langle u_{\text{rel},1}^2 \rangle$ with increasing M_r/M_c in Figure 4 is as follows. First, it should be pointed out that all the five cases A–E are for *two-way coupling* and have the same volume fraction and particle properties. Now, for case A, one computational particle represents 932 real particles, whereas in case E one comp. particle represents only 51 real particles. Therefore in A, the inertia of 932 particles (concentrated in one comp. particle) forces the surrounding fluid to move in the direction of the comp. particle. This directional alignment of the velocities of the particle and fluid reduces $\langle v_{\text{rel},1}^2 \rangle$. In case E, on the other hand, the force of 51 particles is less effective in aligning the fluid velocity with that of the comp. particle. As (M_r/M_c) approaches 1, $\langle v_{\text{rel},1}^2 \rangle$ approaches its real value. It is clear from the figure that this important quantity, $\langle v_{\text{rel},1}^2 \rangle$, which governs the response of a particle to the turbulent motion of the carrier flow is quite sensitive to the value of (M_r/M_c). This problem, to the author's knowledge, has not been examined by users of the Lagrangian approach. One way to study this problem is to compare the results obtained from DNS using $(M_r/M_c) = 1$ with those from the Lagrangian method using $(M_r/M_c) > 1$ for a homogeneous shear flow [12].

3. DNS of Particle-Laden Turbulent Flows

The method of direct numerical simulation (DNS) for particle-laden flows provides a modeling-free, three-dimensional, instantaneous velocity field for the carrier flow in which the trajectories of a large number of particles are computed via Equation (17). DNS has two limitations: one is related to computer technology and the other is related to the equation of particle motion (17) discussed in the preceding

section. The computer limitation is due to the fact that the ratio of the largest to smallest length scales $\ell/\eta \sim R_\ell^{3/4}$. Since turbulence is a three-dimensional, time-dependent phenomenon we need to resolve the motion in these four dimensions. Spatially, if the number of mesh points in one direction is $N_x = \ell/\eta \sim R_\ell^{3/4}$, then in 3D the total number of points needed is $N_x^3 \sim R_\ell^{9/4}$. Similarly, for time-accurate resolution of the smallest scales, the time-step must be small enough for a fluid particle to travel a distance smaller than η. This means that the dimensionless time-step $\Delta t \sim \Delta x$, i.e. a finer mesh requires a smaller Δt. At the other end of the spectrum, we need to resolve times of the order of a life time of the large scale motion, τ_e. During this turnover time, a fluid particle would move a distance $\approx \ell$. Therefore, the total number of time steps for resolving one eddy turnover time is $N_t = \tau_e/\Delta t \approx \ell/\eta \sim R_\ell^{3/4}$. Thus the minimum computational effort (approximately equal to the number of arithmetic operations performed by the computer to integrate the transport equations) of resolving the spatial and temporal behavior of a large eddy is $N_x^3 \times N_t = R_\ell^{9/4} \times R_\ell^{3/4} = R_\ell^3$. For most engineering flows, $R_\ell = 10^3$, hence the computational effort is $\sim 10^9$, and increasing R_ℓ by only one order of magnitude, the effort increases to 10^{12} (for geophysical flows, $R_\ell \approx 10^8$). These requirements are only for one dependent variable, e.g. a velocity component. It is clear that computing all the velocity components and additional scalars like temperature or species for $R_\ell = 10^5$ is beyond present and anticipated computer technology. It is possible at present to solve the full Navier–Stokes equations with 512^3 points on a dedicated massively parallel computer [5], but most DNS computations use 128^3 points especially if the solution for one or two scalars is needed in addition to that of the velocity field. Computer limitations become even more severe due to the presence of the dispersed particles.

Despite the restriction on R_ℓ that can be simulated, there is already strong evidence that many of the main characteristics of these flows are being correctly predicted by DNS at moderate R_ℓ values. Furthermore, current DNS methods are capable of achieving R_ℓ values that are equal to or greater than those observed in laboratory wind tunnels. It is now widely accepted that massively parallel computing provides a promising approach to further extend that range.

Riley and Patterson [29] were the first to present a computer simulation of 'small' particle (diameter and response time are less than the Kolmogorov length and time scales) autocorrelation and mean-square displacement in a numerically integrated, decaying isotropic flow field. The fluid Eulerian velocity field was obtained by direct numerical simulation of turbulence in a cubical volume (32^3 grid points), with an initial microscale Reynolds $R_\lambda = 23$. The trajectories of 432 particles were obtained from the numerical solution of the equation of particle motion including only the Stokes drag.

Squires and Eaton [33] studied particle dispersion in stationary (forced) and decaying isotropic turbulence of six different (response time) particles, with each simulation tracking the trajectories of 4096 particles. McLaughlin [24] computed

particle trajectories in a numerically simulated vertical channel flow, with $16 \times 64 \times 65$ grid points, to study particle deposition on the wall. The equation of motion of the particle included only the Stokes drag and Saffman lift force. It was found that although the magnitude of Saffman lift force was less than that of the component of Stokes drag normal to the wall, the impulse provided by the lift force had a significant effect on particle deposition within the viscous sublayer. The reason is that in this region the normal component of fluid velocity is relatively small. The Saffman lift force tends to trap the particles within the viscous sublayer.

Elghobashi and Truesdell [11, 13] studied the dispersion of solid particles in decaying isotropic turbulence using a numerical grid containing 96^3 points resolving the turbulent motion at the Kolmogorov length scale for a range of microscale Reynolds numbers starting from $R_\lambda = 25$ and decaying to $R_\lambda = 16$. The dispersion characteristics of three different solid particles (corn, copper and glass) injected in the flow, were obtained by integrating the complete equation of particle motion along the instantaneous trajectories of 22^3 particles for each particle type, and then performing ensemble averaging. The three different particles are those used by Snyder and Lumley [32]. Good agreement was achieved between the DNS results and the measured time development of the mean-square displacement of the particles. Some of the significant findings of [13] is summarized below.

(1) The crossing trajectories [35] and the continuity effect [7] associated with it are manifested in the occurrence of negative loops in the Lagrangian velocity autocorrelations of heavier particles in the lateral directions. These negative loops do not exist in zero gravity.
(2) For all particles in gravity environment, the magnitudes of the Lagrangian autocorrelations of the surrounding fluid are less than those of particles, and the higher the response time of the particle, the lower is the autocorrelation of the surrounding fluid.
(3) The 'true' effects of turbulence on solid particle dispersion can be 'seen' only in the lateral directions since the drift velocity can overshadow the turbulent velocity fluctuations.
(4) The theory of Taylor [34] on the turbulent diffusion of fluid points can be applied directly to solid particles in zero gravity. Large deviations from the theory occur for long dispersions times in gravity environment due to the crossing trajectories effect. This effect manifests itself in the decay of the product $\langle u_{pi}^2 \rangle R_\tau$, and not just in the decrease of R_τ.
(5) The inertia of a solid particle may cause its turbulent diffusivity in zero gravity to exceed that of its corresponding fluid point, i.e. the turbulent Schmidt number of a particle in zero gravity is less than unity, for short dispersion times. For long dispersion times, in zero gravity, the diffusivities of both reach asymptotic values, in agreement with Taylor's theory. In gravity environment, and for long times, the turbulent diffusivity of a solid particle, in the lateral directions, decreases monotonically thus eventually increasing its turbulent

Schmidt number by orders of magnitude above that in zero gravity. This reduction of lateral dispersion of the particle at long times is due to both inertia and gravity.

(6) The Lagrangian velocity frequency spectra of the particles in zero gravity show that at low frequencies, the turbulence energy of each of the considered particles exceeds that of the corresponding surrounding fluid. This result contradicts Csanady's theory [7], for the ratio of particle energy to that of the surrounding fluid, when used in decaying turbulence. In gravity environment, the ratio of particle energy to that of the surrounding fluid is frequency sensitive. That is, gravity reduces particle energy at medium and high frequencies, in the lateral directions, below that of the surrounding fluid. The reverse takes place at lower frequencies where particle energy becomes higher than that of the surrounding fluid.

(7) The study of the time development of all the forces acting on a solid particle shows that in the gravity direction the buoyancy and drag forces dominate the particle behavior, and the former may exceed the latter. In the lateral directions, the drag and Basset forces are the main forces although the former is at least one order of magnitude higher than the latter.

Recently, Elghobashi and Truesdell [14] used DNS to study the modification of decaying homogeneous turbulence due to the two-way coupling with dispersed small solid particles ($d/\eta < 1$), at a volumetric loading ratio $\Phi_p \leq 5 \times 10^{-4}$. The results show that the particles increase the fluid turbulence energy at high wave numbers. This increase of energy is accompanied by an increase of the viscous dissipation rate, and hence an increase in the rate of energy transfer $T(k)$ from the large scale motion. Thus, depending on the conditions at particle injection, the fluid turbulence kinetic energy may increase initially. But, in the absence of external sources (shear or buoyancy), the turbulence energy eventually decays faster than in the particle-free turbulence.

In gravitational environment, particles transfer their momentum to the small-scale motion but in an *anisotropic* manner. The pressure-strain correlation acts to remove this anisotropy by transferring energy from the direction of gravity to the other two directions, *but at the same wave number*, i.e. to the small-scale motion in directions normal to gravity. This input of energy in the two directions with lowest energy content causes a *reverse cascade*. This reverse cascade tends to build up the energy level at lower wave numbers, thus reducing the decay rate of energy as compared to that of either the particle-free turbulence or the zero-gravity particle-laden flow.

4. Large Eddy Simulation (LES)

The objective of LES is to resolve the three-dimensional time-dependent details of the largest scales of motion, ℓ, while using simple closure models for the smaller

scales, or *subgrid scales*. The advantage of not fully resolving *all* the scales, as in DNS, is to allow higher Reynolds number flows to be simulated. Thus LES is not limited by computer capabilities as DNS. LES has been used to predict turbulent single-phase flows in simple geometries (e.g. channel with and without sudden expansion) and atmospheric flows. It is possible to use LES at present to predict the dispersion of particles (*one-way coupling*) in simple flows, since particle dispersion is controlled mainly by the large scale motion. However, the main obstacle in employing LES in the *two-way coupling* regime is that the subgrid scales at which closure modeling is required are those where the interaction between the particles and turbulence occurs. Thus, the benefits that would be gained from resolving the large scales accurately would be lost by the approximations of the closure models. However, it is expected that when better closure models become available for the two-way coupling regime, LES would play an important role in predicting high Reynolds number flows in complex geometries.

5. Closing Remarks

The preceding sections review the challenges associated with the task of numerically predicting particle-laden turbulent flows. The review highlighted the progress made in the past few years especially in DNS and in the statistical approach in deriving the dispersed-phase transport equations. Only incompressible, isothermal flows without phase change or particle-particle collision were considered. Suggestions were made for improving closure modeling of some important correlations.

The following remarks can be made:

(1) Turbulence closure models for particle-laden flows are needed (for both the two-fluid and Lagrangian methods) for complex geometries in practical applications due to computer limitations. However, in order to improve the accuracy of these closure models, the detailed physics of the interaction between turbulence and the dispersed particles must be understood.

(2) The Lagrangian method is most suitable for the one-way coupling regime. In order to improve its accuracy in two-way coupling regimes, one must carefully examine the effects of the ratio M_r/M_c. It seems necessary that a pdf for the particle number density needs to be computed in the Lagrangian method before one can accurately predict two-way and four-way coupling regimes due to computer limitations.

(3) The two-fluid method is better suited for predicting two-way and four-way coupling regimes. The statistical approach for deriving the dispersed-phase transport equations is recommended due to its accuracy in evaluating the turbulent fluxes and stresses, e.g. $\langle \phi u_i \rangle_p$ and $\langle u_i u_i \rangle_p$.

(4) DNS can provide otherwise unavailable information about the fine structure of turbulence, particle dispersion and the two-way interaction between par-

ticles and turbulence (modulation of energy and dissipation spectra, velocity autocorrelations for particles and fluid points, etc.).

(5) *Well-defined* experiments with *acceptable* accuracy in simple turbulent flows *should be* coordinated at inception with the numerical simulation. These experiments are needed to extend the applicability domain of DNS.

Acknowledgement

I would like to express my gratitude to Dr. Michael Reeks for his careful review of this article and for many suggestions now incorporated in the text.

References

1. Andresen, E., Statistical approach to continuum models for turbulent gas-particle flows. Ph.D. Dissertation, Technical University of Denmark (1990).
2. Berlemont, A., Desjonqueres, P. and Gouesbet, G., Particle Lagrangian simulation in turbulent flows. *Int. J. Multiphase Flow* 16 (1990) 19–34.
3. Buyevich, Yu. A., Statistical hydromechanics of disperse. Part 2: Solution of the kinetic equation for suspended particles. *J. Fluid Mech.* 52 (1972) 345–355.
4. Chao, B. T., Turbulent transport behavior of small particles in dilute suspension. *Österr. Ing. Arch.* 18 (1964) 7.
5. Chen, S., Doolen, G. D., Kraichnan, R. H. and She, Z. S., On statistical correlations between velocity increments and locally averaged dissipation in homogeneous turbulence. *Phys. Fluids* A5 (1993) 458–463.
6. Crowe, C. T., Chung, J. N. and Trout, T. R., Particle mixing in free shear flows. *Prog. Energy Combust. Sci.* 14 (1988) 171–194.
7. Csanady, G. T., Turbulent diffusion of heavy particles in the atmosphere. *J. Atm. Sci.* 20 (1963) 201–208.
8. Elghobashi, S. E., Particle-laden turbulent flows: direct simulation and closure models. *Appl. Sci. Res.* 48 (1991) 301–314.
9. Elghobashi, S. E. and Abou Arab, T. W., A two-equation turbulence model for two-phase flows. *Phys. Fluids* 26 (1983) 931–938.
10. Elghobashi, S. E., Abou Arab, T. W., Rizk, M. and Mostafa, A., Prediction of the particle-laden jet with a two-equation turbulence model. *Int. J. Multiphase Flow* 10 (1984) 697.
11. Elghobashi, S. E. and Truesdell, G. C., Direct simulation of particle dispersion in a decaying isotropic turbulence. *Seventh Symposium on Turbulent Shear Flows*, Stanford University (1989).
12. Elghobashi, S. E. and Truesdell, G. C., Direct simulation of particle dispersion in grid turbulence and homogeneous shear flows. *Bull. Am. Phys. Soc.* 34 (1989) 2311.
13. Elghobashi, S. E. and Truesdell, G. C., Direct simulation of particle dispersion in decaying isotropic turbulence. *J. Fluid Mech.* 242 (1992) 655–700.
14. Elghobashi, S. E. and Truesdell, G. C., On the two-way interaction between homogeneous turbulence and dispersed solid particles, part 1: turbulence modification. *Phys. Fluids* A5 (1993) 1790–1801.
15. Gosman, A. D. and Ioanides, E., Aspects of computer simulation of liquid-fuelled combustors. *AIAA 19th Aerospace Sciences Meeting, St. Louis, MO*, Paper No. 81-0323 (1981).
16. Hwang, G. J. and Shen, H. H., Modeling the solid-phase stress in a fluid-solid mixture. *Int. J. Multiphase Flow* 15 (1989) 257–268.
17. Kim, I., Elghobashi, S. and Sirignano, W., Three dimensional flow interactions between a cylindrical vortex tube and a spherical particle. *J. Fluid Mech.* (submitted, 1993).
18. Kim, I., Elghobashi, S. and Sirignano, W., Three dimensional flow over two spheres placed side by side. *J. Fluid Mech.* 246 (1993) 465–488.

19. Lopez de Bertodano, M., Lee, S.-J., Lahey, R. T., Jr. and Drew, D. A., The prediction of two-phase turbulence and phase distribution phenomena using a Reynolds stress model. *J. Fluids Eng.* 112 (1990) 107–113.
20. MacInnes, J. M. and Bracco, F. V., Stochastic particle dispersion and the tracer-particle limit. *Phys. Fluids* A4 (1992) 2809–2824.
21. Marble, F. E., Dynamics of gas containing small solid particles. *Proceedings of the 5th AGARD Symposium, Combustion and Propulsion*, Pergamon, New York (1963) pp. 175–215.
22. Maxey, M. R., The equation of motion for a small rigid sphere in a nonuniform or unsteady flow. *ASME-Fluids Eng. Div.* 166 (1993) 57–62.
23. Maxey, M. R. and Riley, J. J., Equation of motion for a small rigid sphere in a nonuniform flow. *Phys. Fluids* 26 (1983) 883–889.
24. McLaughlin, J. B., Aerosol particle deposition in numerically simulated channel flow. *Phys. Fluids* A1 (1989) 1211–1224.
25. McLaughlin, J. B., Inertial migration of a small sphere in linear shear flow. *J. Fluid Mech.* 224 (1991) 261–274.
26. Reeks, M. W., On a kinetic equation for the transport of particles in turbulent flows. *Phys. Fluids* A3 (1991) 446–456.
27. Reeks, M. W., On the continuum equations for dispersed particles in nonuniform flows. *Phys. Fluids* A4 (1992) 1290–1303.
28. Reeks, M. W., On the constitutive relations for dispersed particles in nonuniform flows. 1: Dispersion in a simple shear flow. *Phys. Fluids* A5 (1993) 750–763.
29. Riley, J. J. and Patterson, G. S., Jr., Diffusion experiments with numerically integrated isotropic turbulence. *Phys. Fluids* 17 (1974) 292.
30. Saffman, P. G., The lift on a small sphere in a slow shear flow. *J. Fluid Mech.* 22 (1965) 385–400.
31. Saffman, P. G., The lift on a small sphere in a slow shear flow – corrigendum. *J. Fluid Mech.* 31 (1968) 624.
32. Snyder, W. H. and Lumley, J. L., Some measurements of particle velocity autocorrelation functions in a turbulent flow. *J. Fluid Mech.* 48 (1971) 41.
33. Squires, K. D. and Eaton, J. K., Measurements of particle dispersion obtained from direct numerical simulations of isotropic turbulence. *J. Fluid Mech.* 226 (1991) 1–35.
34. Taylor, G. I., Diffusion by continuous movement. *Proc. Lond. Math. Soc.* A 20 (1921) 196.
35. Yudine, M. I., Physical considerations on heavy-particle diffusion. *Adv. Geophys.* 6 (1959) 185–191.
36. Yuu, S., Yasukouchi, N., Hirosawa, Y. and Jotaki, T., Particle turbulent diffusion in a dust-laden round jet. *J. AIChE* 24 (1978) 509–519.
37. Zhou, Q. and Leschziner, M. A., A time-correlated stochastic model for particle dispersion in anisotropic turbulence. *Eight Symposium on Turbulent Shear Flows* 1 (1991) 1031–1036.